Geophysical Research Letters

RESEARCH LETTER
10.1029/2018GL078789

Key Points:
- The first evaluation of global freshwater availability below normal conditions in +1.5 versus +2 °C worlds is conducted
- Relative to the historical period, future water availability below normal conditions would decrease in the midlatitudes and the tropics
- Risk of freshwater shortages in a +1.5 °C world is less than a +2 °C world

Supporting Information:
- Table S1
- Figure S1

Correspondence to:
F. Sun,
sunfb@igsnrr.ac.cn

Citation:
Liu, W., Lim, W. H., Sun, F., Mitchell, D., Wang, H., Chen, D., et al. (2018). Global freshwater availability below normal conditions and population impact under 1.5 and 2 °C stabilization scenarios. *Geophysical Research Letters*, *45*. https://doi.org/10.1029/2018GL078789

Received 21 MAR 2018
Accepted 26 JUL 2018
Accepted article online 2 AUG 2018

Global Freshwater Availability Below Normal Conditions and Population Impact Under 1.5 and 2 °C Stabilization Scenarios

Wenbin Liu[1], Wee Ho Lim[1,2], Fubao Sun[1,3,4,5], Dann Mitchell[6], Hong Wang[1], Deliang Chen[7], Ingo Bethke[8], Hideo Shiogama[9], and Erich Fischer[10]

[1]Key Laboratory of Water Cycle and Related Land Surface Processes, Institute of Geographic Sciences and Natural Resources Research, Chinese Academy of Sciences, Beijing, China, [2]Environmental Change Institute, University of Oxford, Oxford, UK, [3]Ecology Institute of Qilian Mountain, Hexi University, Zhangye, China, [4]College of Resources and Environment, University of Chinese Academy of Sciences, Beijing, China, [5]Center for Water Resources Research, Chinese Academy of Sciences, Beijing, China, [6]School of Geographical Sciences, University of Bristol, Bristol, UK, [7]Regional Climate Group, Department of Earth Sciences, University of Gothenburg, Gothenburg, Sweden, [8]Uni Research Climate, Bjerknes Centre for Climate Research, Bergen, Norway, [9]Center for Global Environmental Research, National Institute for Environmental Studies, Tsukuba, Japan, [10]Institute for Atmospheric and Climate Science, ETH Zurich, Zurich, Switzerland

Abstract Based on the large ensembles of the half a degree additional warming, prognosis, and projected impacts historical, +1.5 and +2 °C experiments, we quantify changes in the magnitude of water availability (i.e., precipitation minus actual evapotranspiration; a function of monthly precipitation flux, latent heat flux, and surface air temperature) below normal conditions (less than median, e.g., 20th percentile water availability). We found that, relative to the historical experiment, water availability below normal conditions of the +1.5 and +2 °C experiments would decrease in the midlatitudes and the tropics, indicating that hydrological drought is likely to increase in warmer worlds. These cause more (less) people in East Asia, Central Europe, South Asia, and Southeast Asia (West Africa and Alaska/Northwest Canada) to be exposed to water shortage. Stabilizing warming at 1.5 °C instead of 2 °C would limit population impact in most of the regions, less effective in Alaska/Northwest Canada, Southeast Asia, and Amazon. Globally, this reduced population impact is ~117 million people.

Plain Language Summary This study emerges from the lack of scientific investigations to inform climate policy about differences between two global warming targets (i.e., 1.5 and 2 °C) for the "Intergovernmental Panel on Climate Change Special Report on Global Warming of 1.5°C." We seek to understand the following: How would water availability below normal conditions (the drier end of hydrological extremes) change at these targets? How would they affect the water shortage of human society? Could we limit the impact by stabilizing the global warming at 1.5 °C instead of 2 °C? To address these questions, we employ the HAPPI (half a degree additional warming, prognosis, and projected impacts) experiments, explicitly designed to differentiate impacts between these targets. Relative to the historical period, future water availability below normal conditions (less than median, e.g., 20th percentile or lower) would decrease in the midlatitudes and the tropics; the globe and most of the regions would endure water shortages. Relative to the 2 °C warming target, stabilizing temperature increase at 1.5 °C would constrain adverse impact on people suffering water shortages in most of the regions (particularly Central Europe, East Africa, East Asia, South Asia, and West Africa) but ineffective in Alaska/Northwest Canada, Southeast Asia, and Amazon. A global sum of this reduced risk is ~117 million people.

1. Introduction

Securing an adequate freshwater supply (i.e., net of precipitation minus evapotranspiration) is vital for sustaining human activities (e.g., agricultural production, industrial, and domestic water consumptions) and environmental requirements (Falkenmark, 1989; Gudmundsson et al., 2017; Rijsberman, 2006). Whilst the global-mean hydrological cycle is anticipated to intensify with global warming (Lim & Roderick, 2009; Oki & Kanae, 2006; Roderick et al., 2014), the changing distribution of freshwater both spatially and temporally constrains freshwater supply (Liu et al., 2017; Vörösmarty et al., 2010; World Economic Forum, 2015) and risks national food security, economic prosperity, and societal well-being (Mekonnen & Hoekstra, 2016; Rijsberman, 2006), albeit with large uncertainty in the estimated response (Jiménez Cisneros et al., 2014; Prudhomme et al., 2014). To

minimize this uncertainty and help keep hazardous climate extremes to a minimum in an interfered climate system, an official agreement has been reached to hold global warming to less than 2 °C above the preindustrial levels with a possible adoption at 1.5 °C target (UNFCCC Conference of the Parties, 2015).

The lack of scientific literature to inform climate policy about differences between these specified warming targets (i.e., 1.5 and 2 °C) has called for a new form of analyses to support an Intergovernmental Panel on Climate Change (IPCC) special report on "climate impacts of global warming of 1.5°C" in 2018 (Diffenbaugh et al., 2018; Hulme, 2016; Liu et al., 2018; Mitchell et al., 2016; Peters, 2016; Schleussner et al., 2016; Seneviratne et al., 2016). In response to this call and the recent proposal for broadening the definition of drought to include water shortage cause and human-modified processes (Van Loon, 2015; Van Loon et al., 2016), we put forward some relevant questions including the following: How would global water availability below normal conditions (less than median, e.g., 20th percentile or lower, the drier end of hydrological extremes) change at the Paris Agreement global warming targets? How would they affect the water shortage of society? Could we avoid/reduce the impact and risk at 1.5 °C relative to 2 °C? The "event attribution-style" climate experiments —half a degree additional warming, prognosis, and projected impacts (HAPPI)—were explicitly designed to differentiate impacts between these global warming targets. They used large ensembles of equilibrated climate (Mitchell et al., 2017) to allow insight into these questions relative to earlier climate experiments, for example, the Couple Model Intercomparison Project Phase 3 (e.g., Arnell, 2004; Arnell & Lloyd-Hughes, 2014; Fung et al., 2011; Murray et al., 2012), CMIP5 (e.g., Hanasaki et al., 2013), and the Inter-Sectoral Impact Model Intercomparison Project (ISI-MIP; Prudhomme et al., 2014; Schewe et al., 2014; Veldkamp et al., 2016).

Whilst hydrological models are traditionally applied for climate impact assessments, studies have confirmed their weakness in low-flow simulations (de Wit et al., 2007; Smakhtin, 2001; Smakhtin et al., 1998; Stahl et al., 2011). This is caused by poor understanding about hydrological processes under low-flow conditions (Smakhtin, 2001), hence inadequate mathematical representation of hydrological systems (see Gudmundsson et al., 2012, p. 616). This might explain why existing hydrological models are more suitable for wet conditions but not for dry conditions (Stahl et al., 2012; Staudinger et al., 2011). Comprehensive evaluation in the Water Model Intercomparison Project further confirmed large uncertainty in hydrological drought simulations among the large-scale hydrological models (Gudmundsson et al., 2012), which generally exhibit problematic snow and groundwater performances (see details in Van Loon, 2015). Given the above challenges in simulation of the drier end of hydrological extremes, we substitute them with an alternative approach specifically designed to address the questions put forward in this study (above). Without subscribing to a specific statistical distribution, we used a mathematical approach that objectively compare the change in magnitude of water availability below normal conditions among the climate models and with the ability to synthesize the climate models output and the baseline data (details in section 2).

In conjunction with the HAPPI climate models, we use a global hydrological product from a climate data record (CDR) and global population data that are consistent with the United Nation's World Population Prospects (constant 2015; Center for International Earth Science Information Network, 2017; we do not account for future population growth in this study). We evaluate how the magnitude of freshwater availability below normal conditions in the future period (1.5 and 2 °C) would change relative to the historical period. To express its population impact in a comprehensible way (relative to water amount), we apply a water stress indicator (on a per person basis) to estimate the change in affected population due to the change in freshwater shortage between the historical and future periods. We present these results on global and subcontinental scales consistent with the IPCC (2012) and make inferences to previous studies.

2. Data and Methods

2.1. Data

The overall approach of our study is illustrated in Figure S1 in the supporting information. First, we obtain atmosphere-only general circulation models (AGCMs) output of the HAPPI Tier 1 experiments (Bentsen et al., 2013; Lierhammer et al., 2017; Shiogama et al., 2014; Stevens et al., 2013; von Salzen et al., 2013). These experiments do not assume any human activities (e.g., land use and water use) on the water cycle. The Tier 1 experiments consist of multiple perturbed initial condition simulations (50–100 ensemble members per AGCM) for three 10-year periods: (i) a historical period (2006–2015; hereafter referred to as *historical experiment*), (ii) a future period at 1.5 °C above the preindustrial levels (2106–2115; hereafter referred to as

+1.5 °C experiment), and (iii) a future period at 2 °C above the preindustrial levels (2106–2115; hereafter referred to as *+2 °C experiment*). The large number of ensemble members per AGCM allows for multiyear event analysis of extremes (see details in Mitchell et al., 2017). HAPPI is a multimodel project, but we select only the AGCMs that output the following monthly variables: (i) precipitation flux (*pr*, kg m^{-2} s^{-1}), (ii) latent heat flux (*hfls*, W m^{-2}), and (iii) surface air temperature (*tas*, K); in addition, we stipulate that the first 50 ensembles are available for all the Tier 1 experiments. Following this, we use five AGCMs (CanAM4, ECHAM6-3-LR, ETH-CAM4-2degree, MIROC5, and NorESM1-HAPPI) with sufficient samples (50 ensembles × 10 years × 12 months = 6,000 monthly samples per AGCM) per experiment (see Table S1).

We take the summation of runoff and water storage change (includes groundwater, snowmelt, and soil moisture) of the CDR (Zhang et al., 2018) for the global terrestrial water budget (spatial resolution: 0.5° × 0.5°, temporal resolution: monthly, and time period: 1984–2010) to represent the baseline water availability (27 years × 12 months = 324 monthly samples). The CDR is an optimized estimation of the terrestrial water budget through merging in situ observations, satellite remote sensing, reanalysis, and land surface model outputs using data assimilation techniques. The runoff data have been validated against in situ discharge measurements obtained from the Global Runoff Data Centre and the U.S. Geological Survey (Zhang et al., 2018). The water storage change data were the ensemble mean of that prepared by three centers, GeoForschungsZentrum in Potsdam; Center for Space Research at University of Texas, Austin; and Jet Propulsion Laboratory (Zhang et al., 2018).

We apply the recently released Gridded Population of the World, version 4, that was adjusted using United Nation's World Population Prospects (Center for International Earth Science Information Network, 2017; link: http://sedac.ciesin.columbia.edu/data/set/gpw-v4-population-count-adjusted-to-2015-unwpp-country-totals-rev10). Whilst the original spatial resolution of this product is high (i.e., 30″ × 30″), we download the upscaled product at similar spatial resolution as the CDR. To be consistent with the historical period (2006–2015) of the HAPPI archive, we select the population count data in 2015 and keep it constant. Note that we do not apply the population projection of the shared socioeconomic pathways (SSPs) because they were specifically designed for the climate simulations based on representative concentration pathways. It is difficult to reconcile the future period (2106–2115) of the HAPPI archive (originally designed to address climate attribution questions) with the forcing windows of the representative concentration pathways and hence the SSPs projections.

2.2. Methods

2.2.1. Estimate Water Availability Below Normal Conditions

From the AGCMs monthly output (we apply the original spatial resolution), we use the precipitation (*pr*, kg m^{-2} s^{-1}) and latent heat flux (*hfls*, W m^{-2}) to calculate the water availability (Q^*, mm d^{-1}) at each grid cell,

$$Q^* = \frac{86400000}{\rho_W}\left(pr - \frac{hfls}{\lambda_W}\right) \tag{1}$$

where ρ_W (kg m^{-3}) is the density of liquid water (≈1,000 kg m^{-3}) and λ_W (J kg^{-1}) is the latent heat of vaporization. From water balance perspective, Q^* equates the summation of runoff and water storage change (includes groundwater, snowmelt, soil moisture). Typically, the fluctuation of water storage change is significant (small) under nonsteady (steady) state conditions, for example, timescale of less than (at least) a year.

Following Allen et al. (1998), we calculate λ_W as,

$$\lambda_W = 2.501\times10^6 - 2361(tas - 273.15) \tag{2}$$

From these equations, we prepare the water availability for the historical and future periods (i.e., Q^*_{his} and Q^*_{fut}), respectively. The subscript *his* refers to the historical experiment in the historical period, and the subscript *fut* refers to the +1.5 or +2 °C experiment in the future period.

For each AGCM, we construct a cumulative distribution function (CDF) of the monthly water availability Q^* in each grid cell per experiment (e.g., historical, +1.5 °C, and +2 °C experiment). From these CDFs, we use a percentile threshold (e.g., *x*th percentile) as one way to define the water availability below normal conditions for both historical and future periods (i.e., $Q^*_{his,x}$ and $Q^*_{fut,x}$, respectively). We rescale these

estimates to a common spatial resolution (0.5° × 0.5°) using the bilinear interpolation so that we could consistently analyze them. Whilst it is finer than the original spatial resolution of the AGCMs (see Table S1), it enables us to streamline and preserve the spatial details of hydrologic information when synthesizing the baseline data (section 2.1) with the percentile of AGCMs in the water shortage analysis (section 2.2.2 and Figure S1).

To compare these percentiles (previous paragraph), we compute the percentile in the historical period for the water availability $Q^*_{his,(fut,x)}$ corresponding to the future period $Q^*_{fut,x}$ (i.e., the percentile in the historical period equivalent to the magnitude of the xth percentile water availability in the future period). If the computed percentile of $Q^*_{his,(fut,x)}$ is lower (higher) than $Q^*_{fut,x}$, then $Q^*_{fut,x}$ is drier (wetter) than $Q^*_{his,x}$. If the computed percentile of $Q^*_{his,(fut,x)}$ equates $Q^*_{fut,x}$, then $Q^*_{fut,x}$ is identical to $Q^*_{his,x}$.

From literature, we have confirmed that the 20th percentile (Q^*_{20}; a value being equaled or exceeded 80% of the time) is a commonly used threshold in large scale hydrologic investigations (i.e., hydrological drought and water scarcity; Andreadis et al., 2005; Sheffield et al., 2009; van Huijgevoort et al., 2013). Hence, we set x = 20 for our analysis throughout the main text. For each AGCM, we calculate Q^*_{20} at each grid cell (50 ensembles × 10 years × 12 months = 6,000 monthly samples per AGCM) across all experiments (i.e., historical, +1.5 °C, and +2 °C experiments). To generalize them, we calculate the ensemble mean of the percentile in the historical period for the water availability corresponding to the future period ($Q^*_{his,(fut,x)}$, also see previous paragraph) across five AGCMs and show the model consistency in terms of direction change (but not magnitude change). To test the robustness of our findings, we repeat the analysis using lower thresholds (e.g., Q^*_5, Q^*_{10}) in the supporting information. We also performed a separate set of significance testing for a number of percentiles (e.g., Q^*_5, Q^*_{20}, and Q^*_{50}) across all the AGCMs using the Wilcoxon Sign Test (see Figures S4–S6). The Wilcoxon Sign Test is a nonparametric test close to the dependent t test. It does not assume normal distribution for the samples and is useful for analyzing data when the numbers of samples are relatively small (Oliver et al., 2015).

2.2.2. Estimate People Affected by Water Shortage

To streamline all AGCMs projections, we match the CDF of water availability in the historical period per AGCM to that of the baseline (see Section 2.1). Briefly, this CDF mapping technique is common in hydroclimate studies (e.g., Boe et al., 2007; Deque, 2007; Reichle & Koster, 2004; Sun et al., 2011) and is categorized as a form of "distribution mapping" approach (Teutschbein & Seibert, 2012). Whilst this technique applies a similar correction algorithm to both historical and future periods like all bias-correction approaches, comprehensive evaluation has confirmed its merit over other existing approaches (e.g., Liu et al., 2015; Liu & Sun, 2017; Teutschbein & Seibert, 2012). In this way, we could, to some extent, reduce the uncertainties due to individual features of the five AGCMs.

For each AGCM per experiment, we quantify the people affected by water shortage per grid cell $P_{aff,\ grid}$ (unit: person) as

$$P_{aff,grid} = \min\left\{\frac{Q^*_x - D_P \times P_{all,grid}}{D_P}, P_{all,grid}\right\} \tag{3}$$

where Q^*_x ($m^3\ d^{-1}$) is the xth percentile water availability of a specific period (broadly represents the freshwater supply in this study), D_P ($m^3\ person^{-1}\ d^{-1}$) is the water demand threshold and $P_{all,\ grid}$ (person) is the population size per grid cell. We constrain the number of people affected by water shortage per grid cell so that it does not exceed the population size per grid cell ($P_{all,\ grid}$). To calculate Q^*_x, we match the percentile of the AGCM water availability (i.e., historical period: the xth percentile water availability in the historical period, $Q^*_{his,x}$; future period: the percentile in the historical period for the water availability corresponding to the xth percentile of that in the future period, $Q^*_{his,(fut,x)}$; we set x = 20 with that of the baseline in order to get the CDR water availability. Following the Falkenmark water stress indicator (e.g., Falkenmark, 1989, 2013), we set the water demand threshold (D_P) equivalent to 1,700 and 1000 $m^3\ person^{-1}\ yr^{-1}$, respectively. We aggregate the people affected by water shortage per grid cell $P_{aff,\ grid}$ to subcontinental and global scales and calculate the change in affected population from the historical period to the future period (i.e., Δ ($fut_{+1.5}$ − his), Δ ($fut_{+2.0}$ − his); Note: Positive [negative] number means that the number of people adversely affected by water shortage would increase [decrease]). When presenting these estimates (details in section 3.2), we exclude the grid cells where both historical and future periods do not encounter water shortages.

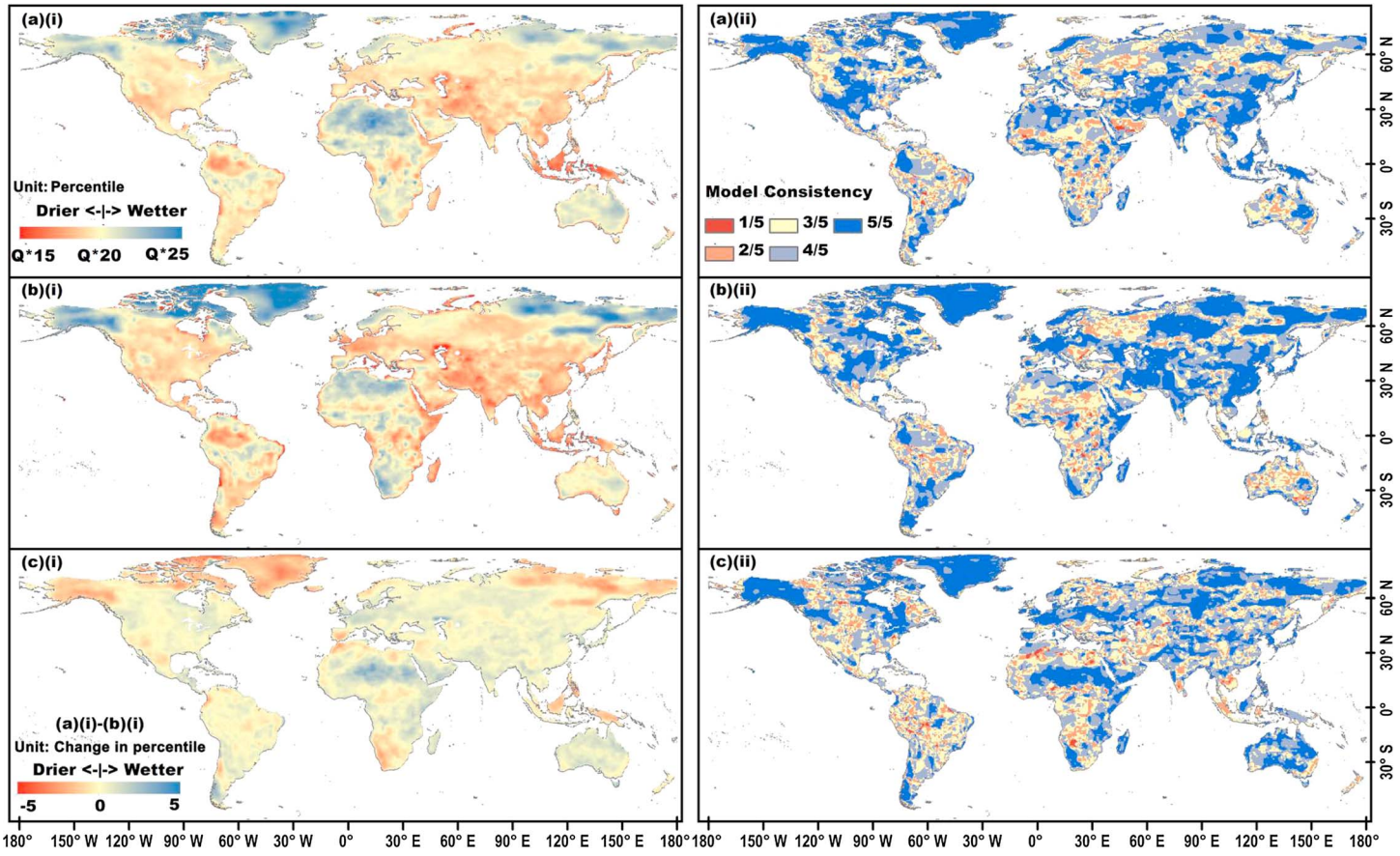

Figure 1. Multimodel ensemble mean percentile in the historical period for monthly water availability corresponding to the future period Q^*_{20} (i) and model consistency (ii) on a spatial resolution of 0.5° × 0.5° for (a) +1.5 °C experiment; (b) +2 °C experiment; and (c), (a) minus (b). The percentile $<Q^*20$ ($>Q^*20$) indicates that magnitude of the future period Q^*_{20} would decrease (increase). Robustness of projections increases with higher model consistency and vice versa. Legend in (a)(i) applies to (b)(i); legend in (a)(ii) applies to (b)(ii) and (c)(ii).

3. Results

3.1. Projections of Water Availability Below Normal Conditions

The multimodel ensemble mean (MEM) percentile in the historical period for monthly water availability corresponding to the future period Q^*_{20} shows some robust large-scale features (Figure 1). For the +1.5 °C experiment, there is some indication that the 20th percentile water availability would increase at very high latitudes in the Northern Hemisphere, and in the Sahara. More strongly, the simulations indicate a decrease (i.e., drying) in the 20th percentile water availability in the midlatitudes (e.g., Central Asia, West Asia and East Asia, and middle and south of North America) and the tropics (e.g., parts of Amazon basin, north of Chile, southeastern Brazil, Malaysia, Indonesia, Thailand, Cambodia, Vietnam, Laos, New Guinea, Kenya, Tanzania, Gabon, and Congo and Democratic Republic of Congo). Whilst the geographic pattern of changes in the 20th percentile water availability for the +2 °C experiment is close to that of +1.5 °C experiment, the magnitude of both positive and negative changes intensifies in most of the regions, except for the Sahara, Malaysia, and Indonesia. We repeat a similar process at lower thresholds (Q^*_{10}, Q^*_5) and find that the spatial pattern of the changes (drier/wetter) are insensitive to the threshold (whilst the magnitude would vary; Figures S2–S3), confirming the robustness of these projections. More generally, these results imply that the magnitude of droughts arising from water availability below normal conditions would be less severe in most parts of the world should we pursue climate change mitigation efforts to hold temperature increase at 1.5 °C instead of 2 °C above the preindustrial levels.

Most of the spatial patterns are consistent with previous studies despite different climate experiments and/or methods used (Alcamo et al., 2007; Hagemann et al., 2013; Lehner et al., 2017; Schleussner et al., 2016).

Specifically, the decrease in the 20th percentile water availability in Europe, Middle East, southwestern United States, and Central America coincides with an analysis using CMIP5 experiment output and offline river routing (Koirala et al., 2014).

The high intermodel consistency on the sign of change (3–5 models within 5 AGCMs) in most of the regions for the future periods (+1.5 and +2 °C experiments and their difference; see Figure 1(ii)) gives us some confidence on these projections. All models indicate that drought risk associated with water availability below normal conditions would intensify when global warming approaches the 2 °C (instead of 1.5 °C) above the preindustrial levels. (The Wilcoxon Sign Test confirms that the regions where most of the AGCMs showed statistically significant results (e.g., see hatching in Figure S5) are close to the outcomes of the intermodel consistency in Figure 1(ii).)

Following the definition of regions in the IPCC (2012), we reorganize these projections and estimate the global and regional mean of MEM percentile in the historical period for monthly water availability corresponding to the future period Q^*_{20} (Figure 2). Globally, the MEM of the magnitude of the 20th percentile water availability is projected to increase slightly (from Q^*_{20} to $Q^*_{20.10}$) under +1.5 °C experiment whilst barely changing (from Q^*_{20} to $Q^*_{20.03}$) under +2 °C experiment relative to the historical experiment, indicating that differences between +1.5 and +2 °C experiments are not statistically robust or nonlinear effects play an important role. Regionally, the MEMs of the 20th percentile water availability would decrease under the +1.5 °C experiment, except for West Africa (from Q^*_{20} to $Q^*_{20.35}$), South Africa (from Q^*_{20} to $Q^*_{20.11}$), Sahara (from Q^*_{20} to $Q^*_{21.72}$), Northern Europe (from Q^*_{20} to $Q^*_{20.17}$), North Australia (from Q^*_{20} to $Q^*_{20.76}$), North Asia (from Q^*_{20} to $Q^*_{20.32}$), East Canada, Greenland, Iceland (from Q^*_{20} to $Q^*_{21.86}$), Alaska/Northwest Canada (from Q^*_{20} to $Q^*_{21.00}$) and South Australia/New Zealand (from Q^*_{20} to $Q^*_{20.16}$). The direction of changes in MEM of the 20th percentile water availability is quite similar under the +2 °C experiment, except for South Australia/New Zealand, Northern Europe, and West Africa. Relative to the 2 °C warming target, a 1.5 °C warming target is more likely to reduce drought risk triggered by water availability below normal conditions globally and regionally (except for the Southeast Asia, South Africa, North Asia, Southern Europe and Mediterranean, East Canada, Greenland, Iceland, and Alaska/Northwest Canada. Notably, increasing water availability at very high latitudes in the Northern Hemisphere is positive for glacier accumulation, e.g., Alaska/East Canada/Greenland [Figure S6]).

In some regions, the projections are subject to a large spread across the ensemble, for example, Southeast Asia, Sahara, and Northeastern Brazil. The spread owing to differences between AGCMs is evident in South Australia/New Zealand, Northern Europe, and Southern Africa, where AGCMs project the 20th percentile water availability changes are of opposite sign. However, the changes in MEM of the 20th percentile water availability in Southern Africa (slight increase) under different warming periods agree with the hydrological drought changes projected by Prudhomme et al. (2014) using ISI-MIP experiments.

3.2. Population Impact

To understand the population impact of water availability below normal conditions, we reconcile the projections (Q^*_{20}) with population distribution information (constant 2015) in order to estimate the people affected by water shortage between the historical (baseline results in Figure S8) and future periods (Figures S9 and S11). At the water demand threshold level of 1,700 m^3 $person^{-1}$ yr^{-1}, the number of people adversely affected by water shortage in +1.5 and +2 °C experiments would increase by ~3.7% (~271 million) and ~5.3% (~388 million) of global population relative to the historical period (Table S2), respectively. These are consistent with the expectation of elevating water stress/scarcity in a warmer climate (Liu et al., 2017; Veldkamp et al., 2016). The benefit of holding global warming at 1.5 °C instead of 2 °C above the preindustrial levels is apparent in most of the regions (e.g., East Asia, South Asia, Central Europe, West Africa, and East Africa).

From regional aggregation, we find that more (less) people in East Asia, South Asia, Central Europe, and Southeast Asia (West Africa and Alaska/Northwest Canada) would be exposed to the risk of water shortage under the future periods.

Our projections suggest that stabilizing temperature increase at 1.5 °C instead of 2 °C would constrain adverse impact on people suffering water shortages in most of the regions (particularly Central Europe, East Africa, East Asia, South Asia, and West Africa) but less effective in Alaska/Northwest Canada, Southeast

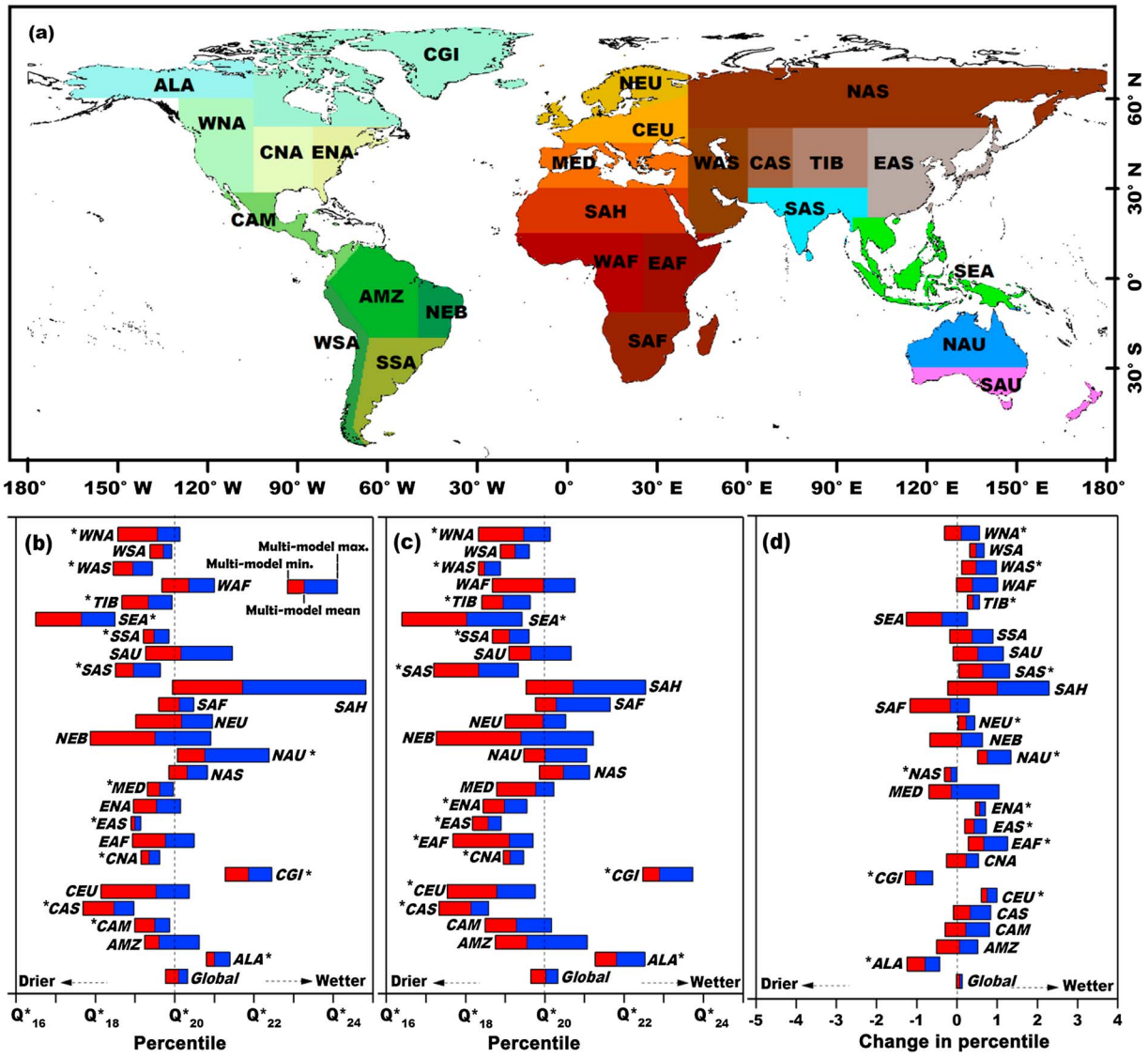

Figure 2. Multimodel mean percentile in the historical period for monthly water availability corresponding to the future period Q^*_{20} in different regions (a) for (b) +1.5 °C experiment; (c) +2 °C experiment; and (d), (b) minus (c). These boxplots are prepared using five models. The color bar in (b)–(d) shows the multimodel maximum (blue), multimodel minimum (red), and multimodel ensemble mean (the dividing line between blue and red colors). The percentile $<Q^*20$ ($>Q^*20$) indicates that magnitude of the future period Q^*_{20} would decrease (increase). Legend in (b) applies to (c) and (d). The asterisks in (b)–(d) indicate that changes in percentile are significant according to a Wilcoxon Sign Test (95% confidence).

Asia, and Amazon basin. Globally, we estimate the reduction in adversely affected population (when limiting the warming to 1.5 °C rather than 2 °C) to be ~117 million people. Repeating this analysis using the water demand threshold 1,000 m^3 $person^{-1}$ yr^{-1}, we confirm that the spatial distribution (Figures S10 and S12) of water shortage appears similar to that using 1,700 m^3 $person^{-1}$ yr^{-1}. In a sense, both thresholds confirm that there is a clear advantage of holding global warming at 1.5 °C relative to 2 °C above the preindustrial levels.

4. Discussions

This study is performed using five AGCMs from the HAPPI consortium that fulfill our selection criteria. The HAPPI experimental design enables generation of large ensembles (Mitchell et al., 2016), making it particularly suitable for identification of changing patterns of extreme hydrological events such as droughts driven by water availability below normal conditions (e.g., Q^*_5, Q^*_{10}, and Q^*_{20}). The findings presented in this

study supplement the drought/low-flow studies prepared using earlier climate modeling archives (CMIP5 and ISI-MIP; e.g., Koirala et al., 2014; Prudhomme et al., 2014; Schewe et al., 2014; Schleussner et al., 2016) but are specific to the global warming targets put forward by the Paris Agreement, and their differences (if any) compared to the standard climate projection approaches (e.g., Mitchell et al., 2016). By concentrating our analysis on these targets, it is possible for international policymakers to comprehend societal impact of water shortages triggered by freshwater availability below normal conditions on global and regional scales.

Based on constant population count, the estimated number of people affected by the 20th percentile water availability (Tables S2–S3) is in fact a function of where in space those water shortages occur. Hence, our estimates are subject to uncertainty arising from spatial population and climate covariability. Nonetheless, the results of the last section might not sufficiently address the uncertainty arising from climate variability of each ensemble member. Recent demonstrations (e.g., Deser et al., 2012; Hawkins & Sutton, 2011; Mankin et al., 2017; Mankin & Diffenbaugh, 2015) have shown that the concept of signal-to-noise (S/N) ratio can be applied to compare the magnitude of the mean of a specific number of trends (signal) to the standard deviation of those trends (noise). The signal (S) is robust when the S/N ratio exceeds 1. Following this concept, for each of the 50 ensembles (see first paragraph in section 2.1) in the future period (i.e., +1.5 and +2 °C experiments), we calculate the percentile in the historical period (i.e., historical experiment) for monthly water availability corresponding to the 20th percentile in the future period. We determine the signal (S) as the magnitude of the mean of these 50 percentiles, and noise (N) as the standard deviation of these percentiles; and subsequently derive the S/N ratio. We repeat the calculation for all five AGCMs. The outcomes (Figure S7) confirm that the projections of the 20th percentile water availability in the future period are robust across all AGCMs, suggesting that uncertainty arising from undersampling climate variability is generally small considering the large ensemble sizes (per AGCM) in HAPPI archive.

Given the robustness of these projections (Figure S7), it would be interesting to understand the variability in drying/wetting pattern of the 20th percentile water availability among the AGCMs (Figure S5). The AGCMs show consistent drying/wetting pattern in some regions (e.g., northern America and eastern/southeastern/southern Asia) but uncertain in other regions (e.g., the central part of South America and southern Africa). Similar analysis for the 5th percentile water availability (Figure S4) yields similar pattern (in terms of direction change) among the AGCMs as Figure S5. Repeating this analysis for the 50th percentile water availability (Figure S6), the drying/wetting pattern shifts (e.g., more variation in eastern/southeastern/southern Asia). These outcomes (Figures S4–S6) indicate that the drying/wetting patterns of the water availability below normal conditions (e.g., between 5th and 20th percentile) is not applicable to the higher percentiles.

The estimates presented here are based on raw AGCMs water availability Q^* (i.e., precipitation minus actual evapotranspiration, which covers the runoff, groundwater, and snowmelt), avoiding uncertainties due to structural weakness of low-flow simulation within many existing hydrological models (Van Loon, 2015). Furthermore, the need of removing spin-up period from the relatively short duration of HAPPI experiments (2006–2015 and 2106–2115) makes it much less preferable to apply hydrological modeling tools. Since these estimates are consistent with recent global studies (e.g., Koirala et al., 2014), despite the simplicity of our methodology, they adequately capture the large-scale freshwater shortage patterns.

The calculation of freshwater supplies below normal conditions here prioritized societal water requirements over the environmental water requirements. It implicitly excludes the role of existing freshwater storages (e.g., freshwater lakes, dams, reservoirs) in regulating the freshwater supply (mostly replenished during normal and above normal conditions, e.g., wet season). Estimates of water demand here made use of thresholds (e.g., 1,700 and 1,000 m^3 $person^{-1}$ yr^{-1}) of the Falkenmark water stress indicator. The shortcomings are its inability to reflect local water scarcities, availability of infrastructure which modifies water supplies (e.g., dams, reservoirs, and river diversion) or how representative it is for countries with differences in lifestyle and climate conditions (Rijsberman, 2006). It remains a challenge to understand and account for the uncertainty of water requirements due to human activities and its potential atmospheric feedback (Jaramillo & Destouni, 2015; Keune et al., 2018). Despite these limitations, it is commonly applied to large-scale investigations (e.g., Schewe et al., 2014; Veldkamp et al., 2016), mainly because of its simplicity and broad account for water requirement covering household, agricultural, industrial, energy sector, and the environment

(Falkenmark, 1989, Rijsberman, 2006). This is probably because it serves as a good proxy to gauge adequacy of water supply to meet the demand of the society on macroscales. The baseline data (i.e., CDR) applied in current study are an optimized product of multiple hydrologic data sources, hence inherited some uncertainty, which might need further refinement. When better hydrologic products become available in the future, it is possible to use our methodology (Figure S1) to estimate the population impact with higher confidence.

5. Summary

The newly released HAPPI experiments enable us, for the first time, to present a global assessment of changes for range of water availability below normal conditions (i.e., Q^*_{20}, Q^*_{10}, and Q^*_5) and subsequent population impact under 1.5 and 2 °C warming scenarios. We found that the MEM of water availability below normal conditions would decrease in most of the regions (particularly in the midlatitudes and the tropics) except for Sahara and many very high northern latitude regions (>70°N) in +1.5 and +2 °C experiments. We confirmed the benefit of holding global warming at 1.5 °C instead of 2 °C above the preindustrial levels, with less severe decrease in water availability below normal conditions across most of the regions (except for Southeast Asia, South Africa, North Asia, Southern Europe and Mediterranean, East Canada, Greenland, Iceland, and Alaska/Northwest Canada) and the globe. At the 20th percentile water availability conditions Q^*_{20}, our estimation suggested that more population would suffer from water shortage in most of the regions in 1.5 and 2 °C warming worlds. By stabilizing warming to 1.5 °C instead of 2 °C above the preindustrial levels, the number of people affected by water shortage at water availability below normal conditions would be lesser in many regions, that is, Central Europe, East Africa, East Asia, South Asia, and West Africa. These findings addressed the questions raised earlier and should provide science-based evaluation on the benefit of holding 1.5 °C warming (in the water sector) and inform climate policy. Future efforts involving population growth (e.g., SSPs), hydrologic simulation (when low-flow simulation advances), and water infrastructure (e.g., dams, reservoirs, and river diversion canals) at finer scales would help in addressing the local climate adaptation and water management strategies.

Acknowledgments
The research was supported by the National Key Research and Development Program of China (2016YFA0602402 and 2016YFC0401401), the Key Research Program of the Chinese Academy of Sciences (ZDRW-ZS-2017-3-1), and the CAS Pioneer Hundred Talents Program (Fubao Sun). W. H. L. acknowledge funding support from the CAS President's International Fellowship Initiative (2017PC0068). D. C. was supported by CAS (XDA20060401) as well as Swedish VR and STINT. H. S. was supported by Integrated Research Program for Advancing Climate Models. D. M. was supported by a NERC independent research fellowship (NE/N014057/1). I. B. was supported by the Research Council of Norway (261821) and Sigma2 (ns9082k). This research used science gateway resources of the National Energy Research Scientific Computing Center, a DOE Office of Science User Facility supported by the Office of Science of the U.S. Department of Energy under contract DE-AC02-05CH11231. We thank all our colleagues involving in HAPPI experiments. We thank the editor and two anonymous reviewers for helpful comments. All the data used in the article are available in the references provided and the supporting information.

References

Alcamo, J., Flörke, M., & Märker, M. (2007). Future long-term changes in global water resources driven by socio-economic and climatic changes. *Hydrological Sciences Journal*, *52*(2), 247–275. https://doi.org/10.1623/hysj.52.2.247

Allen, R. G., Pereira, L. S., Raes, D., & Smith, M. (1998). Crop evapotranspiration—Guidelines for computing crop water requirements. FAO Irrigation and Drainage Paper 56, Rome, Italy. Retrieved from https://appgeodb.nancy.inra.fr/biljou/pdf/Allen_FAO1998.pdf

Andreadis, K. M., Clark, E. A., Wood, A. W., Hamlet, A. F., & Lettenmaier, D. P. (2005). Twentieth-century drought in the conterminous United States. *Journal of Climate*, *6*(6), 985–1001. https://doi.org/10.1175/JHM450.1

Arnell, N. W. (2004). Climate change and global water resources: SRES emissions and socio-economic scenarios. *Global Environmental Change*, *14*(1), 31–52. https://doi.org/10.1016/j.gloenvcha.2003.10.006

Arnell, N. W., & Lloyd-Hughes, B. (2014). The global-scale impacts of climate change on water resources and flooding under new climate and socio-economic scenarios. *Climatic Change*, *122*(1-2), 127–140. https://doi.org/10.1007/s10584-013-0948-4

Bentsen, M., Bethke, I., Debernard, J. B., Iversen, T., Kirkevåg, A., Seland, Ø., et al. (2013). The Norwegian Earth System Model, NorESM1-M—Part 1: Description and basic evaluation of the physical climate. *Geoscientific Model Development*, *6*(3), 687–720. https://doi.org/10.5194/gmd-6-687-2013

Boe, J., Terray, L., Habets, F., & Martin, E. (2007). Statistical and dynamical downscaling of the Seine basin climate for hydro-meteorological studies. *International Journal of Climatology*, *27*(12), 1643–1655. https://doi.org/10.1002/joc.1602

CIESIN (2017). Gridded Population of the World, Version 4 (GPWv4): Population count adjusted to match 2015 revision of UN WPP country totals, revision 10. Palisades, New York: NASA Socioeconomic Data and Applications Center (SEDAC). https://doi.org/10.7927/H4JQ0XZW, Accessed: 20 April 2018.

Deque, M. (2007). Frequency of precipitation and temperature extremes over France in an anthropogenic scenario: Model results and statistical correction according to observed values. *Global and Planetary Change*, *57*(1-2), 16–26. https://doi.org/10.1016/j.gloplacha.2006.11.030

Deser, C., Philips, A., Bourdette, V., & Teng, H. (2012). Uncertainty in climate change projections: The role of internal variability. *Climate Dynamics*, *38*(3-4), 527–546. https://doi.org/10.1007/s00382-010-0977-x

Diffenbaugh, N. S., Singh, D., & Mankin, J. S. (2018). Unprecedented climate events: Historical changes, aspirational targets, and national commitments. *Science Advances*, *4*, eaao3354. https://doi.org/sciadv.aao3354

Falkenmark, M. (1989). The massive water scarcity now threatening Africa: Why isn't it being addressed? *Ambio*, *18*(2), 112–118. Retrieved from https://www.jstor.org/stable/4313541

Falkenmark, M. (2013). Growing water scarcity in agriculture: Future challenge to global water security. *Philosophical Transactions of the Royal Society A*, *371*, 20120410. https://doi.org/10.1098/rsta.2012.0410(2002)

Fung, F. A., Lopez, A., & New, M. (2011). Water availability in +2°C and + 4°C worlds. *Philosophical Transactions of the Royal Society A*, *369*(1934), 99–116. https://doi.org/10.1098/rsta.2010.0293

Gudmundsson, L., Seneviratne, S. I., & Zhang, X. (2017). Anthropogenic climate change detected in European renewable freshwater resources. *Nature Climate Change*, *7*(11), 813–816. https://doi.org/10.1038/nclimate3416

Gudmundsson, L., Tallaksen, L. M., Stahl, K., Clark, D. B., Dumont, E., Hagemann, S., et al. (2012). Comparing large-scale hydrological model simulations to observed runoff percentiles in Europe. *Journal of Hydrometeorology*, *13*(2), 604–620. https://doi.org/10.1175/JHM-D-11-083.1

Hagemann, S., Chen, C., Clark, D. B., Folwell, S., Gosling, S. N., Haddeland, I., et al. (2013). Climate change impact on available water resources obtained using multiple global climate and hydrology models. *Earth System Dynamics*, *4*(1), 129–144. https://doi.org/10.5194/esd-4-129-2013

Hanasaki, N., Fujimori, S., Yamamoto, T., Yoshikawa, S., Masaki, Y., Hijioka, Y., et al. (2013). A global water scarcity assessment under shared socio-economic pathways—Part 2: Water availability and scarcity. *Hydrology and Earth System Sciences*, *17*(7), 2393–2413. https://doi.org/10.5194/hess-17-2393-2013

Hawkins, E., & Sutton, R. (2011). The potential to narrow uncertainty in projections of regional precipitation change. *Climate Dynamics*, *37*(1-2), 407–418. https://doi.org/10.1007/s00382-010-0810-6

van Huijgevoort, M. H. J., Hazenberg, P., van Lanen, H. A. J., Teuling, A. J., Clark, D. B., Folwell, S., et al. (2013). Global multimodel analysis of drought in runoff for the second half of the twentieth century. *Journal of Hydrometeorology*, *14*(5), 1535–1552. https://doi.org/10.1175/JHM-D-12-0186.1

Hulme, M. (2016). 1.5°C and climate research after the Paris Agreement. *Nature Climate Change*, *6*(3), 224–228. https://doi.org/10.1038/nclimate2938

IPCC (2012). *Managing the risk of extreme events and disasters to advance climate change adaptation. A special report of working groups I and II of the Intergovernmental Panel on Climate Change*. Cambridge: Cambridge University Press. Retrieved from https://www.ipcc.ch/pdf/special-reports/srex/SREX_Full_Report.pdf

Jaramillo, F., & Destouni, G. (2015). Local flow regulation and irrigation raise global human water consumption and footprint. *Science*, *350*(6265), 1248–1251. https://doi.org/10.1126/science.aad1010

Jiménez Cisneros, B. E., Oki, T., Arnell, N. W., Benito, G., Cogley, J. G., Döll, P., et al. (2014). *Freshwater resources In: Climate Change 2014: Impacts, adaptation and vulnerability part A: Global and sectoral aspects. Contribution of working group II to the fifth assessment report of the Intergovernmental Panel on Climate Change*. Cambridge: Cambridge University Press. Retrieved from https://www.ipcc.ch/pdf/assessment-report/ar5/wg2/WGIIAR5-Chap3_FINAL.pdf

Keune, J., Sulis, M., Kollet, S., Siebert, S., & Yoshihide, W. (2018). Human water use impacts on the strength of the continental sink for atmospheric water. *Geophysical Research Letters*, *45*, 4068–4076. https://doi.org/10.1029/2018GL077621

Koirala, S., Hirabayashi, Y., Mahendran, R., & Kanae, S. (2014). Global assessment of agreement among streamflow projections using CMIP5 model outputs. *Environmental Research Letters*, *9*(6), 064017. https://doi.org/10.1088/1748-9326/9/6/064017

Lehner, F., Coats, S., Stocker, T. F., Pendergrass, A. G., Sanderson, B. M., Raible, C. C., & Smerdon, J. E. (2017). Projected drought risk in 1.5°C and 2°C warmer climates. *Geophysical Research Letters*, *44*, 7419–7428. https://doi.org/10.1002/2017GL074117

Lierhammer, L., Mauritsen, T., Legutke, S., Esch, M., Wieners, K.-H., & Saeed, F. (2017). Simulations of HAPPI (half a degree additional warming, prognostic and projected impacts) Tier-1 experiments based on the ECHAM6.3 atmospheric model of the max Planck Institute for Meteorology (MPI-M). *World Data Center for Climate (WDCC) at DKRZ*. Retrieved from http://cera-www.dkrz.de/WDCC/ui/Compact.jsp?acronym=HAPPI-MIP_ECHAM6.3

Lim, W. H., & Roderick, M. L. (2009). *An atlas of the global water cycle: Based on the IPCC AR4 climate models*. Canberra: ANU Epress. http//press.anu.edu.au?p=127241, https://doi.org/10.26530/OAPEN_458809

Liu, J., Yang, H., Gosling, S. N., Kummu, M., Flörke, M., Pfister, S., et al. (2017). Water scarcity assessments in the past, present and future. *Earth's Future*, *5*(6), 545–559. https://doi.org/10.1002/2016EF000518

Liu, W. B., & Sun, F. (2017). Projecting and attributing future changes of evaporative demand over China in CMIP5 climate models. *Journal of Hydrometeorology*, *18*(4), 977–991. https://doi.org/10.1175/JHM-D-16-0204.1

Liu, W. B., Sun, F., Lim, W. H., Zhang, J., Wang, H., Shiogama, H., et al. (2018). Global drought and severe drought-affected populations in 1.5 and 2°C warmer worlds. *Earth System Dynamics*, *9*(1), 267–283. https://doi.org/10.5194/esd-9-267-2018

Liu, W. B., Zhang, A., Wang, L., Fu, G., Chen, D., Liu, C., & Cai, T. (2015). Projecting streamflow in the Tangwang River basin (China) using a rainfall generator and two hydrological models. *Climate Research*, *62*(2), 79–97. https://doi.org/10.3354/cr01261

Mankin, J. S., & Diffenbaugh, N. S. (2015). Influence of temperature and precipitation variability on near-term snow trends. *Climate Dynamics*, *45*(3-4), 1099–1116. https://doi.org/10.1007/s00382-014-2357-4

Mankin, J. S., Viviroli, D., Mekonnen, M. M., Hoekstra, A. Y., Horton, R. M., Smerdon, J. E., & Diffenbaugh, N. S. (2017). Influence of internal variability on population exposure to hydroclimatic changes. *Environmental Research Letters*, *12*(4), 044007. https://doi.org/10.1088/1748-9326/aa5efc

Mekonnen, M. M., & Hoekstra, A. Y. (2016). Four billion people facing severe water scarcity. *Science Advances*, *2*(2), e1500323. https://doi.org/10.1126/sciadv.1500323

Mitchell, D., AchutaRao, K., Allen, M., Bethke, I., Beyerle, U., Ciavarella, A., et al. (2017). Half a degree additional warming, prognosis and projected impacts (HAPPI): Background and experimental design. *Geoscientific Model Development*, *10*(2), 571–583. https://doi.org/10.5194/gmd-10-571-2017

Mitchell, D., James, R. J., Forster, P. M., Betts, R. A., Shiogama, H., & Allen, M. (2016). Realizing the impacts of a 1.5°C warmer world. *Nature Climate Change*, *6*(8), 735–737. https://doi.org/10.1038/nclimate3055

Murray, S. J., Forster, P. N., & Prentice, I. C. (2012). Future global water resources with respect to climate change and water withdrawals as estimated by a dynamic global vegetation model. *Journal of Hydrology*, *448-449*, 14–29. https://doi.org/10.1016/j.jhydrol.2012.02.044

Oki, T., & Kanae, S. (2006). Global hydrological cycles and world water resources. *Science*, *313*(5790), 1068–1072. https://doi.org/10.1126/science.1128845

Oliver, T. H., Marshall, H. H., Morecroft, M. D., Brereton, T., Prudhomme, C., & Huntingford, C. (2015). Interacting effects of climate change and habitat fragmentation on drought-sensitive butterflies. *Nature Climate Change*, *5*(10), 941–945. https://doi.org/10.1038/nclimate2746

Peters, G. P. (2016). The "best available science" to inform 1.5°C policy choices. *Nature Climate Change*, *6*(7), 646–649. https://doi.org/10.1038/nclimate3000

Prudhomme, C., Giuntoli, I., Robinson, E. L., Clark, D. B., Arnell, N. W., Dankers, R., et al. (2014). Hydrological droughts in the 21st century, hotspots and uncertainties from a global multimodel ensemble experiment. *Proceedings of the National Academy of Sciences of the United States of America*, *111*(9), 3262–3267. https://doi.org/10.1073/pnas.1222473110

Reichle, R. H., & Koster, R. D. (2004). Bias reduction in short records of satellite soil moisture. *Geophysical Research Letters*, *31*, L19501. https://doi.org/10.1029/2004GL020938

Rijsberman, F. R. (2006). Water scarcity: Fact or fiction? *Agricultural Water Management*, *80*(1-3), 5–22. https://doi.org/10.1016/j.agwat.2005.07.001

Roderick, M. L., Sun, F., Lim, W. H., & Farquhar, G. D. (2014). A framework for understanding the response of the water cycle to global warming over land and ocean. *Hydrology and Earth System Sciences*, *18*(5), 1575–1589. https://doi.org/10.5194/hess-18-1575-2014

von Salzen, K., Scinocca, J. F., McFarlane, N. A., Li, J. N., Cole, J. N. S., Plummer, D., et al. (2013). The Canadian fourth generation atmospheric global climate model (CanAM4) – Part I: Representation of physical processes. *Atmosphere-Ocean*, *51*(1), 104–125. https://doi.org/10.1080/07055900.2012.755610

Schewe, J., Heinke, J., Gerten, D., Haddeland, I., Arnell, N. W., Clark, D. B., et al. (2014). Multimodel assessment of water scarcity under climate change. *Proceedings of the National Academy of Sciences of the United States of America*, *111*, 3245–3250. https://doi.org/10.1073/pnas.1222460110

Schleussner, C.-F., Lissner, T. K., Fischer, E. M., Wohland, J., Perrette, M., Golly, A., et al. (2016). Differential climate impacts for policy-relevant limits to global warming: The case of 1.5°C and 2°C. *Earth System Dynamics*, *7*(2), 327–351. https://doi.org/10.5194/esd-7-327-2016

Seneviratne, S. I., Donat, M. G., Pitman, A. J., Knutti, R., & Wilby, R. L. (2016). Allowable CO2 emissions based on regional and impact-related climate targets. *Nature*, *529*(7587), 477–483. https://doi.org/10.1038/nature16542

Sheffield, J., Andreadis, K. M., Wood, E. F., & Lattenmaier, D. P. (2009). Global and continental drought in the second half of the twentieth century: Severity-area-duration analysis and temporal variability of large-scale events. *Journal of Climate*, *22*(8), 1962–1981. https://doi.org/10.1175/2008JCLI2722.1

Shiogama, H., Watanabe, M., Imada, Y., Mori, M., Kamae, Y., Ishii, M., & Kimoto, M. (2014). Attribution of the June-July 2013 heat wave in the southwestern United States. *Scientific Online Letters on the Atmosphere*, *10*, 122–126. https://doi.org/10.2125/sola.2014-025

Smakhtin, V. U. (2001). Low flow hydrology: A review. *Journal of Hydrology*, *240*(3-4), 147–186. https://doi.org/10.1016/S0022-1694(00)00340-1

Smakhtin, V. Y., Sami, K., & Hughes, D. A. (1998). Evaluating the performance of a deterministic daily rainfall-runoff model in a low-flow context. *Hydrological Processes*, *12*(5), 797–812. https://doi.org/10.1002/(SICI)1099-1085(19980430)12:5<797::AID-HYP632>3.0.CO;2-S

Stahl, K., Tallaksen, L. M., Gudmundsson, L., & Christensen, J. H. (2011). Streamflow data from small regions: A challenging test to high-resolution regional climate modeling. *Journal of Hydrometeorology*, *12*(5), 900–912. https://doi.org/10.1175/2011JHM1356.1

Stahl, K., Tallaksen, L. M., Hannaford, J., & van Lanen, H. A. J. (2012). Filling the while space on maps of European runoff trends: Estimates from a multi-model ensemble. *Hydrology and Earth System Sciences*, *16*(7), 2035–2047. https://doi.org/10.5194/hess-16-2035-2012

Staudinger, M., Stahl, K., Seibert, J., Clark, M. P., & Tallaksen, M. (2011). Comparison of hydrological model structures based on recession and low flow simulations. *Hydrology and Earth System Sciences*, *15*(11), 3447–3459. https://doi.org/10.5194/hess-15-3447-2011

Stevens, B., Giorgetta, M., Esch, M., Mauritsen, T., Crueger, T., Rast, S., et al. (2013). Atmospheric component of the MPI-M Earth System Model: ECHAM6. *Journal of Advances in Modeling Earth Systems*, *5*(2), 146–172. https://doi.org/10.1002/jame.20015

Sun, F., Roderick, M. L., Lim, W. H., & Farquhar, G. D. (2011). Hydroclimatic projections for the Murray-Darling Basin based on an ensemble derived from Intergovernmental Panel on Climate Change AR4 climate models. *Water Resources Research*, *47*, W00G02. https://doi.org/10.1029/2010WR009829

Teutschbein, C., & Seibert, J. (2012). Bias correction of regional climate model simulations for hydrological climate-change impact studies: Review and evaluation of different methods. *Journal of Hydrology*, *456-457*, 12–29. https://doi.org/10.1016/j.jhydrol.2012.05.052

UNFCCC Conference of the Parties. (2015). Adoption of the Paris Agreement FCCC/CP/2015/10Add.1 1–32 Paris.

Van Loon, A. F. (2015). Hydrological drought explained. *WIREs Water*, *2*(4), 359–392. https://doi.org/10.1002/wat2.1085

Van Loon, A. F., Gleeson, T., Clark, J., Van Dijk, A. I. J. M., Stahl, K., Hannaford, J., et al. (2016). Drought in the anthropocene. *Nature Geoscience*, *9*(2), 89–91. https://doi.org/10.1038/ngeo2646

Veldkamp, T. I. E., Wada, Y., Aerts, J. C. J. H., & Ward, P. J. (2016). Towards a global water scarcity risk assessment framework: Incorporation of probability distributions and hydro-climatic variability. *Environmental Research Letters*, *11*(2), 024006. https://doi.org/10.1088/1748-9326/11/2/024006

Vörösmarty, C. J., McIntyre, P. B., Gessner, M. O., Dudgeon, D., Prusevich, A., Green, P., et al. (2010). Global treats to human water security and river biodiversity. *Nature*, *467*(7315), 555–561. https://doi.org/10.1038/nature09440

de Wit, M. J. M., van den Hurk, B., Warmerdam, P. M. M., Torfs, P. J. J. F., Roulin, E., & van Deursen, P. A. (2007). Impact of climate change on low-flows in the river Meuse. *Climatic Change*, *82*(3-4), 351–372. https://doi.org/10.1007/s10584-006-9195-2

World Economic Forum (2015). Global Risks 2015 10th Edition (Geneva: World Economic Forum). Retrieved from https://reports.weforum.org/global-risks-2015/

Zhang, Y., Pan, M., Sheffield, J., Siemann, A. L., Fisher, C. K., Liang, M. L., et al. (2018). A climate data record (CDR) for the global terrestrial water budget: 1984-2010. *Hydrology and Earth System Sciences*, *22*(1), 241–263. https://doi.org/10.5194/hess-22-241-2018